Tunable Ultrashort Laser Pulses Generated through Filamentation in Gases

Francis Théberge,[1] Neset Aközbek,[2] Weiwei Liu,[1] Andreas Becker,[3] and See Leang Chin[1]

[1]*Centre d'Optique, Photonique et Laser (COPL), and Département de physique, de génie physique et d'optique, Université Laval, Québec, Québec G1K 7P4, Canada*

[2]*Time Domain Corporation, Cummings Research Park, 7057 Old Madison Pike, Suite 250 Huntsville, Alabama 35806, USA*

[3]*Max-Planck-Institut für Physik komplexer Systeme, Nöthnitzer Strasse 38, D-01187 Dresden, Germany*

(Received 23 February 2006; published 14 July 2006)

Tunable and stable ultrashort laser pulses in the visible spectrum are generated with high efficiency by four-wave mixing process during the filamentation of near-infrared and infrared laser pulses in gases. It is shown that these tunable ultrashort pulses have a very low energy fluctuation and an excellent mode quality due to the processes of intensity clamping and self-filtering in the filament.

DOI: 10.1103/PhysRevLett.97.023904 PACS numbers: 42.65.Re, 42.60.Jf, 42.65.Jx

Nowadays, intense ultrashort laser pulses are a basic tool in many branches of physics and chemistry. They are used, for example, for pump-probe measurements with high time resolution [1], the generation of single attosecond pulses [2], or double-slit interferometry on the attosecond time scale [3]. Experiments in photochemistry and photobiology often additionally require tunability of the central wavelength over a broad spectral range. While few-cycle pulses in the near infrared have been generated, high energy few-cycle coherent sources in the visible spectral region are still lacking. In this Letter we report that such pulses with high beam quality and energy stability can be generated by four-wave mixing during filamentation of an intense near-infrared laser pulse. We obtain 12 fs tunable laser pulses in the visible spectrum with high conversion efficiency by simply recompressing temporally the generated four-wave mixing pulse with a prism compressor. Because of intensity clamping and spatial self-filtering of the pulse during filamentation, the beam parameters are very close to a diffraction limited Gaussian beam and the energy fluctuation is stabilized during the nonlinear propagation.

Filamentation of ultrashort laser pulses in optical media is governed by the dynamic interplay between the optical Kerr effect due to the intensity-dependent refractive index and defocusing from a low-density plasma induced by multiphoton/tunnel ionization (for recent reviews, see Ref. [4]). The defocusing effect of the self-generated plasma balances the self-focusing effect and leads to a limited peak intensity of about 5×10^{13} W/cm^2 during the laser pulse propagation in air [5,6]. This is known as intensity clamping. According to the slice-by-slice self-focusing scenario [7] or the dynamic spatial replenishment model [8], the series of self-foci gives rise to the perception of a filament.

Two recent results led us to expect that the desired goal of a tunable few-cycle laser pulse can be achieved on the basis of laser pulse filamentation. First, it has been shown that the intensity inside the filament is sufficiently high to induce third-harmonic generation [9]. Indeed, the fundamental and the third-harmonic pulses are found to be coupled inside the filament due to a nonlinear phase-locking effect, which results in a phase matching over long propagation distances. It has been expected that the same mechanism holds for all other parametric processes [4], in particular, the third-order four-wave mixing (4WM) process [9]. Second, it has been demonstrated [10] that filamentation of infrared femtosecond pulses in gases leads to a self-compression of the pulse to a few cycles, potentially even to the single-cycle limit [11].

Hence, one may anticipate that tunable ultrashort laser pulses can be generated through four-wave mixing during filamentation and self-compression of infrared laser pulses in gases. This is indeed the case as our experiment shows. It was performed using a Ti:sapphire chirped pulse amplification laser system, which generates femtosecond laser pulses with a central wavelength at 807 nm, a repetition rate of 1 kHz, an energy per pulse of 2 mJ, and a transform-limited pulse duration of 45 fs at full width at half maximum (FWHM). We used a beam splitter to separate the near-infrared (NIR) laser beam into two pulses of equal energy. One pulse was focused into air (or argon gas) at ambient pressure using an 82 cm focal length concave mirror to generate a filament of about 3 cm long. The second pulse was used to pump an optical parametric amplifier (OPA). The pulse duration of the infrared (IR) idler and signal pulses from the OPA was between 75 and 100 fs (FWHM), and the energy per pulse was between 5 and 80 μJ for the central wavelengths ranging between 1.1 and 1.6 μm (signal) and 1.6 mm and 2.4 μm (idler). The IR seed pulse was superposed concentrically with the NIR laser pulse by the use of a dichroic beam splitter positioned before the concave mirror. The temporal delay between the IR and the NIR laser pulses was controlled by an optical delay line.

Because of the strong nonlinear interaction between the IR and the NIR laser pulses during their copropagation, efficient third-order parametric effects occurred within the filament zone. In the present experiment we concentrated on the difference-frequency 4WM process of the IR laser pulse with the NIR fundamental pulse. The output frequency of the generated pulse is determined by

$\omega_{4WM} = 2\omega_{NIR} - \omega_{IR}$, giving rise to visible ultrashort pulses in the range of 475 to 650 nm. Beyond the filament, a dichroic mirror was used to suppress the NIR pulse and to transmit the efficiently generated 4WM pulse. The tunable pulse was then collimated by a plano-convex lens and temporally recompressed by a prism compressor. The pulse duration was measured with a first order interferometric autocorrelator using a 30 μm thick pellicle beam splitter to minimize the group velocity dispersion.

Figure 1(a) shows the conversion efficiency of the generated 4WM pulse in air and argon gas for different IR seed pulses. Constant conversion efficiencies from the IR seed pulse to the 4WM pulse of about 25% and 40% are obtained in air and in argon gas, respectively, by using seed beams in the wavelength range between 1.1 and 1.6 μm. Argon and air have similar third-order susceptibility [12]; the increased 4WM conversion efficiency of Ar results from the higher intensity reached in the filament. For the longer infrared wavelengths, the pulse duration of the IR seed pulse lengthened and the temporal distribution of the IR seed pulse could not be totally superposed with the short NIR pulse generating the filament. As a result, the conversion efficiencies decreased to 5% and 10% for the range of wavelength between 1.6 and 2.4 μm. However, the energy of the generated 4WM pulse exceeded 1 μJ for all IR wavelengths. Figure 1(b) shows the normalized spectra of the 4WM pulses generated in air across the tuning range. Each of the spectra is close to a Gaussian distribution, and they were similar for air and argon gas.

Pulse compression of the generated 4WM beam at the optimum delay for the output energy has been performed using isosceles Brewster-angle fused silica prism pair (60° apex angle) with 77% throughput for double-pass transmission. Using the 82 cm focal length concave mirror to generate the filament, Fig. 2(a) shows a typical spectrum for the 4WM pulse. The measured bandwidth is 23 nm (FWHM), and the calculated transform-limited pulse duration of 22 fs (FWHM) supported by the normalized spectrum is shown in Fig. 2(b). As a comparison, the distribution of the intensity envelope measured with the interferometric autocorrelator is shown in Fig. 2(c). The inferred 23 ± 2 fs pulse duration corresponds to the transform-limited pulse duration.

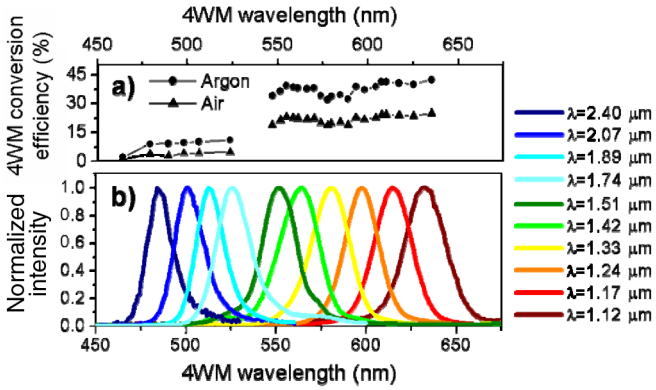

FIG. 1 (color online). (a) 4WM Conversion efficiency in air (▲) and in argon (●) defined as the ratio in percentage of the 4WM pulse energy divided by the input IR seed energy. (b) Generated 4WM pulse spectra with the IR seed (λ) superposed in the filament zone.

During the filamentation the spectral broadening of the NIR laser pulse develops progressively along the self-induced plasma column in air. This means that the longer the filament is, the larger the spectral broadening will be in the emerging pulse [13]. Because of the copropagation of the pump and the IR seed pulse, we expect that the same holds for the 4WM pulse. Figure 2(d) shows the spectral distribution of the generated 4WM pulse when the NIR laser beam was focused in air with a 4 m focal length concave mirror. In this second set of experiments, the length of the plasma column was about 10 times longer (30 cm long) and the 4WM pulse energy was larger than 10 μJ for a 70 μJ IR seed pulse centered at 1.32 μm. As expected the spectrum of the generated 4WM pulse is broadened to 64 nm [Fig. 2(d)]. Figure 2(e) shows the 9 fs transform-limited pulse calculated from the normalized spectrum assuming a flat spectral phase. Because of the broad spectrum, third-order dispersion from the optics could not be compensated totally with the prism compressor, and as shown in Fig. 2(f), we obtained in the experiment a pulse duration of 12 ± 2 fs, which is slightly longer than the transform-limited pulse duration.

The tunable ultrashort 4WM pulses show a remarkable low energy fluctuation and possess an excellent mode quality. Figure 3 shows the temporal evolution of the

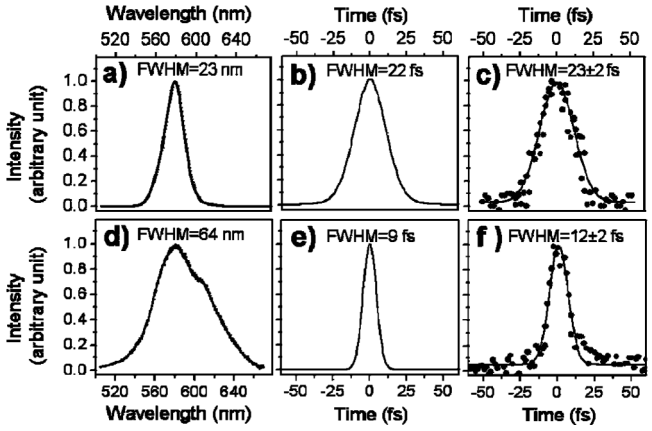

FIG. 2. Results for the 4WM generated pulse during the filamentation in air of a NIR laser beam and a 1.32 mm IR seed beam focused with an 82 cm focal length concave mirror (first row) and a 4 m focal length concave mirror (second row). (a),(d) Normalized 4WM pulse spectrum; (b),(e) the transform-limited pulse duration supported by the normalized spectrum; (c),(f) temporal intensity profile of compressed 4WM pulse as measured from the envelope of the interferometric autocorrelation. The solid line in (c) and (f) are the Gaussian fits of the experimental results.

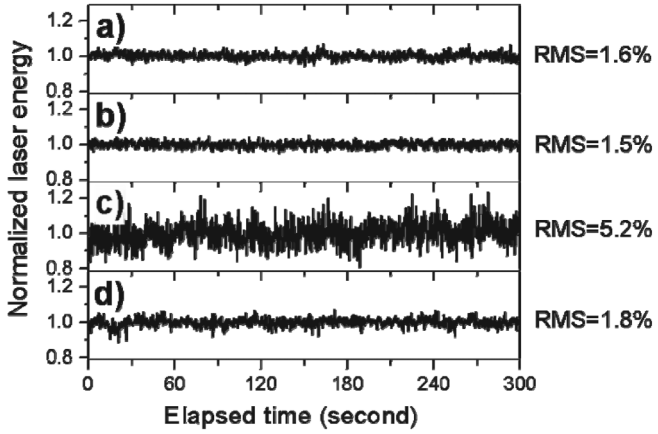

FIG. 3. Temporal evolution of energy per pulse normalized over the mean energy for (a) the IR seed, (b) the NIR pulse, (c) the generated 4WM pulse for NIR pump power (P_{NIR}) 10 times below the critical power for self-focusing (P_{cr}) in air, and (d) the generated 4WM pulse for pump power above the critical power for self-focusing in air ($P_{\mathrm{NIR}} = 2.5P_{\mathrm{cr}}$). The rms energy fluctuations are indicated on the right-hand side.

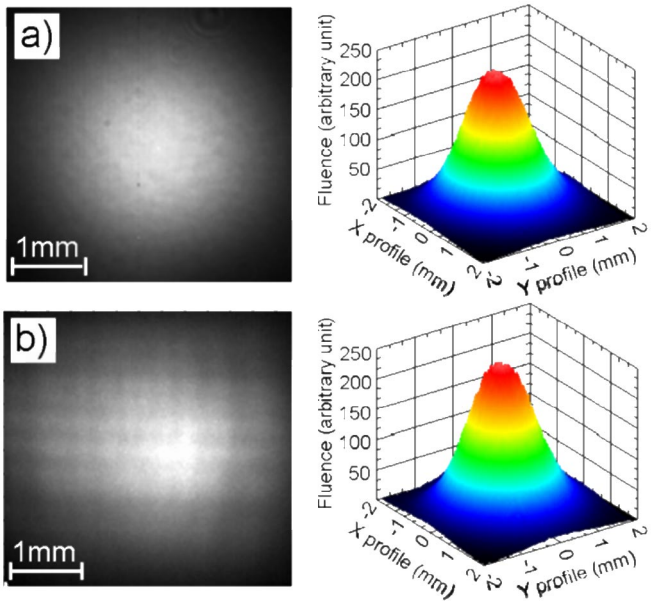

FIG. 4 (color online). Examples of NIR fluence distribution (left) used to generate the filament in air and the far-field fluence distribution of the generated 4WM pulse (right) at a pump power of $2.5P_{\mathrm{cr}}$ are shown in (a) for the undistorted NIR beam and (b) for the NIR beam passing through a square aperture. The ratio $\pi w_0\theta/\lambda$ of the 4WM beam was independent of the initial pump beam profile and below 1.01.

measured laser pulse energies normalized to the mean energy for the IR seed [Fig. 3(a)], NIR [Fig. 3(b)], and the generated 4WM pulses using NIR pump power lower and higher than the critical power for self-focusing [Fig. 3(c) and 3(d), respectively]. The rms energy fluctuation of the input IR and NIR pulses was 1.6% and 1.5%, respectively. In the perturbative limit, one would expect a minimum rms energy fluctuation for the generated 4WM pulse $\mathrm{rms}_{4\mathrm{WM}} = 2 \times \mathrm{rms}_{\mathrm{NIR}} + \mathrm{rms}_{\mathrm{IR}} \cong 4.6\%$. This is indeed close to the measured value of $\mathrm{rms}_{4\mathrm{WM}} = 5.2\%$ for a NIR pump power 10 times below the critical power for self-focusing in air [Fig. 3(c)]. The measured value was slightly higher than the estimated limit because of pulse duration fluctuation and beam pointing wondering of both the NIR and IR laser pulses. But, as we increased the NIR pump power above the critical power for self-focusing in air, we observed a stabilization of the 4WM energy fluctuation [Fig. 3(d)] and measured a rms fluctuation of $\mathrm{rms}_{4\mathrm{WM,fil}} = 1.8\%$, which is 3 times lower than the perturbative limit. The stabilization of the 4WM energy is due to the clamping of the intensity inside the filament. As a consequence, even a large fluctuation of the initial NIR energy results in constant NIR laser intensity inside the filament. We estimate the maximum intensity fluctuation of the NIR pulse inside the filament from $\mathrm{rms}_{\mathrm{NIR,fil}} = (\mathrm{rms}_{4\mathrm{WM,fil}} - \mathrm{rms}_{\mathrm{IR}})/2 = (1.8\%–1.6\%)/2$ to be about 0.1%. Note that the energy fluctuation of the IR seed pulse was not reduced during its propagation because its peak power was much lower than the critical power for self-focusing in air.

Figure 4(a) shows the NIR fluence distribution and the exceptional beam quality profile of the 4WM pulse generated through filamentation. The 4WM fluence distribution was smooth, centered on the propagation axis and similar to a symmetric Gaussian profile. In the case of filamentation, the laser beam profile beyond the filament is different from the initial beam profile due to nonlinear effects. Thus, the standard technique to characterize the M^2 quality factor of the 4WM beam by measuring the beam parameters on either side of a focus is not applicable. It is worth noting that the 4WM pulse developed along the filament, and to characterize its beam quality at the end of the filament, we compared its waist radius (w_0) and far-field divergence (θ) with a diffraction limited Gaussian beam. To cease the nonlinear propagation at the end of the filament, we decoupled the NIR and the 4WM laser pulses with a dichroic mirror. The end of the filament corresponds to the waist of the 4WM beam, and by measuring the beam profile at different distances, we obtained the far-field divergence of the 4WM beam. The product of the measured 4WM beam parameters ($w_0\theta$) divided by λ/π, the latter being the beam parameters product of a diffraction limited Gaussian beam, was below 1.01 in two orthogonal directions. This ratio, close to the theoretical limit of 1, indicates that the parameters of the 4WM beam diffracting out of the filament are very similar to those of a near diffraction limited Gaussian beam whose M^2 value is less than 1.01 while the initial quality factor for the NIR beam was $M^2 = 1.21$. The excellent laser profile of the generated 4WM pulse is due to the spatial self-filtering process occurring in the filament. For laser pulses having

power higher than the critical power for self-focusing, the transverse profile of the beam evolves into a circularly symmetric high constant (clamped) intensity zone surrounded by a background of light (energy reservoir) [14,15]. Even if the initial beam profile and the energy reservoir surrounding the filament core are spatially noisy or asymmetric, the laser intensity distribution in the core of the filament turns into a smooth and circular profile with quasiconstant diameter due to the self-focusing and the self-action of the plasma generation. Since the 4WM pulse is mainly generated in the high intensity zone of the filament, the 4WM pulse acquires a profile similar to the intensity distribution of the NIR pulse inside the filament independent of the initial NIR and IR beam profiles.

To substantiate this interpretation we have verified the influence of the initial NIR laser beam profile on the far-field 4WM beam profile. Thus we have used distorted fluence distributions for the NIR beam profile to generate the filament. The distortions were introduced by diffracting the NIR beam through a square aperture [Fig. 4(b)]. The 8×8 mm^2 square aperture was centered on the beam propagation axis and positioned 3 m before the concave mirror. The NIR energy decreased by 10% by passing through the square aperture, and the corresponding quality factor for the NIR beam was $M^2 = 1.3$. Figure 4(b) shows the diffraction pattern of the NIR beam taken in front of the concave mirror, and we observe multiple peaks distributed along a square grid. For this strongly distorted NIR beam profile we measured again in Fig. 4(b) the same exceptional ratio $\pi w_0 \theta / \lambda$ below 1.01 for the measured 4WM beam diverging out of the filament. Hence due to the spatial self-filtering and intensity clamping processes there is an extraordinary robustness of the beam quality of the generated 4WM pulse. This in turn implies the excellent beam quality of the filament core. Similar results were obtained when the NIR pulse was clipped with a razor blade. It is important to point out that if multiple filaments are generated, each filament will generate its own 4WM beam that may interfere with each other and strongly decrease the quality of the 4WM beam profile in the far-field. However, the use of diffraction phenomena based upon periodic amplitude modulation of the transverse beam profile could be used with high pump power to control the multiple filamentation process [16] and generate in the far-field a matrix of 4WM beams with good quality profiles.

In conclusion, we have demonstrated the efficient generation of powerful and tunable ultrashort laser pulse in the visible spectrum with a simple method through four-wave mixing during the filamentation of femtosecond laser pulses. A wide tuning range across the visible spectrum is achieved and the often encountered limiting factor of material damage is not an issue in the current case using gases. The excellent mode quality and high energy stability are the results of the rich dynamics behind the self-focusing and intensity clamping occurring during filamentation. These natural schemes of stabilization and spatial self-filtering observed in 4WM can be extrapolated to any intensity-dependent process during the filamentation in a transparent medium. We expect that this method could be extended to the generation of few-cycle pulses in the ultraviolet to the midinfrared spectral region by using the appropriate pump sources. Experimental studies in photochemistry, photobiology, and other emerging fields may benefit from the properties of this tunable few-cycle laser source.

We acknowledge the support in part by NSERC, DRDC-Valcartier, FQRNT, Canada Research Chairs, CFI, and CIPI.

[1] A. H. Zewail, J. Phys. Chem. **100**, 12 701 (1996).
[2] M. Hentschel *et al.*, Nature (London) **414**, 509 (2001).
[3] F. Lindner *et al.*, Phys. Rev. Lett. **95**, 040401 (2005).
[4] S. L. Chin *et al.*, Can. J. Phys. **83**, 863 (2005).
[5] H. R. Lange *et al.*, Phys. Rev. Lett. **81**, 1611 (1998).
[6] J. Kasparian, R. Sauerbrey, and S. L. Chin, Appl. Phys. B **71**, 877 (2000).
[7] A. Brodeur *et al.*, Opt. Lett. **22**, 304 (1997).
[8] M. Mlejnek, E. M. Wright, and J. V. Moloney, Opt. Lett. **23**, 382 (1998).
[9] N. Aközbek *et al.*, Phys. Rev. Lett. **89**, 143901 (2002).
[10] C. P. Hauri *et al.*, Appl. Phys. B **79**, 673 (2004).
[11] A. Couairon *et al.*, Opt. Lett. **30**, 2657 (2005).
[12] J. W. Hahn and E. S. Lee, J. Opt. Soc. Am. B **12**, 1021 (1995).
[13] F. Théberge *et al.*, Appl. Phys. B **81**, 131 (2005).
[14] M. Mlejnek, M. Kolesik, J. V. Moloney, and E. M. Wright, Phys. Rev. Lett. **83**, 2938 (1999).
[15] W. Liu *et al.*, Opt. Lett. **30**, 2602 (2005).
[16] V. P. Kandidov *et al.*, Appl. Phys. B **80**, 267 (2005).